KfK 4826
Februar 1991

CHF-KfK-3: A Critical Heat Flux Correlation for Triangular Arrays of Rods with Tight Lattices

M. Dalle Donne
Institut für Neutronenphysik und Reaktortechnik
Projekt Nukleare Sicherheitsforschung

Kernforschungszentrum Karlsruhe

KERNFORSCHUNGSZENTRUM KARLSRUHE
Institut für Neutronenphysik und Reaktortechnik
Projekt Nukleare Sicherheitsforschung

KfK 4826

CHF-KFK-3: A CRITICAL HEAT FLUX CORRELATION FOR TRIANGULAR ARRAYS OF RODS WITH TIGHT LATTICES

M. Dalle Donne*)

*) Delegated from Euratom to the Karlsruhe Nuclear Research Center
Institute for Neutron Physics and Reactor Engineering

Kernforschungszentrum Karlsruhe GmbH, Karlsruhe

Kernforschungszentrum Karlsruhe GmbH
Postfach 3640, 7500 Karlsruhe 1

ISSN 0303-4003

CHF-KFK-3: Eine kritische Heizflächenbelastungskorrelation für Stabbündel in dreieckiger Anordnung und enger Stabteilung

Zusammenfassung

Hochkonvertierende DWR's (HKDWR oder FDWR) basieren auf Brennelementen mit Stäben in einer dreieckigen Anordnung mit enger Stabteilung. Die für solche Geometrie bei KfK früher entwickelte DNB-Korrelation (CHF-KFK-2 Korrelation) ist gegenüber den Experimenten, die vor kurzem durchgeführt wurden, getestet worden. Der Vergleich mit Siemens-KWU Experimenten mit Stabbündeln mit Gitterabstandshaltern und Abstandshaltern mit sechs wendelförmigen integralen Rippen erlaubte, diese frühere Korrelation zu verbessern und zu erweitern. Eine neue Korrelation, CHF-KFK-3 genannt, die diese Verbesserungen berücksichtigt, wird im Bericht vorgestellt.

CHF-KFK-3: A CRITICAL HEAT FLUX CORRELATION FOR TRIANGULAR ARRAYS OF RODS WITH TIGHT LATTICES.

by M. Dalle Donne
Kernforschungszentrum Karlsruhe
Institut für Neutronenphysik und Reaktortechnik

Abstract

High converting PWRS's (HCPWR or APWR) are based on fuel elements with rods placed in a tight lattice triangular array. The CHF correlation developed previously at KfK for such geometry (CHF-KFK-2 correlation) has been tested against recently performed experiments. The comparison with the Siemens-KWU experiments with rod clusters with spacer grid and six integral spiral ribs supports has allowed to improve and extend the previous correlation. A new correlation, called CHF-KFK-3, which accounts for these improvements, is presented in the paper.

CHF-KFK-3: A CRITICAL HEAT FLUX CORRELATION FOR TRIANGULAR ARRAYS OF RODS WITH TIGHT LATTICES.

I. INTRODUCTION

The Karlsruhe Nuclear Research Center and Siemens Kraftwerk Union, in collaboration with the Technical University of Braunschweig and PSI Würenlingen, are studying the possibility of increasing the conversion ratio of a pressurized light water reactor (PWR) in order to improve uranium utilization [1-3]. Similar investigations are being performed in Japan, France and United States as well[4]. For this kind of reactor, called sometimes High Converting Pressurized Water Reactor (HCPWR) or Advanced Pressurized Water Reactor (APWR), the water volume fraction in the core is smaller than in a PWR, thus the neutron spectrum becomes harder and the conversion ratio higher. For this reason the fuel rod lattice in the core is tighter than in a PWR. Generally a triangular rod lattice is chosen, rather than a quadratic one as in the PWR, as this allows a greater minimum gap distance between the fuel rods, for the same water to fuel rod volume ratio. This means that the Critical Heat Flux (CHF) correlations developed for a PWR core geometry are not directly applicable to the case of a APWR core. In the present paper a new, improved CHF correlation is presented, which accounts for the newest experimental results obtained for rod bundles relevant to the APWR-core geometry.

II. THE PREVIOUS CHF-KFK CORRELATIONS

In 1982 Dalle Donne and Hame developed a CHF correlation valid for triangular arrays of rod bundles with tight lattices (CHF-KFK-1)[5]. Subsequently, in 1984 this correlation was improved on the base of the experimental evidence available at that time (CHF-KFK-2)[6]. These correlations were based on the WSC-2 correlation developed by Bowring for various core geometries, however for bundles with relatively wide rod lattices[7]. Table I shows the WSC-2 correlation for the case of bundles with a triangular lattice. The WSC-2 correlation uses British thermal units. These will be retained in the present paper as most of the correlations from the literature quoted here are in those units. The Appendix provides a Nomenclature and unit conversion factors of the physical parameters.

In the WSC-2 correlation Q_1,Q_2,Q_3,Q_4 are the geometry-dependent parameters, while the parameter V accounts for the effect of the bundle spacers. For the best fit of the experimental data with grid spacers, Bowring[7] suggests using the constant value 0.7for V. Dalle Donne and Hame[5,6] determined these parameters anew by root mean-square fitting of experimental data of CHF tests performed for rod bundles with tight triangular lattices ($1.02 < p/d < 1.36$, see Ref. 8,9 and 10). The aim of their work, as well as of the present work, is to produce a CHF correlation valid for the central coolant channels of a cluster. Generally, the burnout does not occur in the wall or corner channels of the fuel rod cluster, because there the water temperature is lower than in the central channels. Mass velocity G in Refs. 8.9 and 10 is the average for the whole bundle, including wall and corner channels. Because the number of rods in these tests is relatively small, the effect of the wall and corner channels could be significant. Dalle Donne and Hame decided therefore to correct the given average $\bar{G}$ values to obtain G values for the central channels of the clusters. Assuming uniform water density, constant friction factors, and equal pressure drop in the various coolant channels, they obtained the correction factor

$$F_G = \frac{G}{\bar{G}} = \frac{(nA + n_w A_w + n_c A_c)\sqrt{D_h}}{nA\sqrt{D_h} + n_w A_w \sqrt{D_{hw}} + n_c A_c \sqrt{D_{hc}}} \qquad (1)$$

where

n = number of central channels

n_w = number of wall channels

n_c = number of corner channels

A = cross-section area of the central channels

Aw = cross-section area of the wall channels

A_c = cross-section area of the corner channels

D_h = hydraulic diameter of the central channels

D_{hw} = hydraulic diameter of the wall channels

D_{hc} = hydraulic diameter of the corner channels

For the data used to obtain the correlation proposed, the F_G values always differed $<7\%$ from unity. For the data from Columbia University, it was assumed $F_G = 1$, because the hydraulic diameters of the corner and wall channels were about the same as that of the central channels, furthermore the strong radial coolant mixing caused by the spiral spacers ensured that the mass velocity is the same in the various coolant channels.

The new values determined by Dalle Donne and Hame[6] were:

$$Q_1 = 1.748, Q_2 = 7.540, Q_4 = 8.783 \qquad (2)$$

whereby Q_3 remains unchanged ($Q_3 = -1$).

And for clusters with grid spacers:

$$V = -0.252 - 2.789 \exp(-3.874\,G) + 1.915 \exp(-0.234\,G) \qquad (3)$$

while for spiral wire spacers:

$$V = 1\text{-}FF\,(0.336 + 0.09G - 0.697 \exp(-2.68G)) \qquad (4)$$

with

$$FF = 2.6695\,(F^{0.915}-1) \qquad (5)$$

$$F = \left(\frac{p}{d}\right)^{0.5} + \left[7.6\,\frac{(p/d)^3}{H/d}\right]^{2.16} \qquad (6)$$

where d = rod diameter, p = rod pitch, H = axial pitch of the spiral spacer.

In the correlation of Ref. /6/ the parameter Y' (see Table I) was omitted because the correlation was intended for application to large bundles with a great number of rods, where the effect of the bundle boundary is negligible on the central rods of the bundle, and in presence of small power gradients perpendicular to the water flow. In this case Y' = 1. However when this correlation is compared with experimental values obtained for bundles with a small number of rods and/or large power gradients across the bundle cross section, a subchannel analysis of the data with a COBRA-type computer code should be performed and the parameter Y' applied.

The correlation obtained by Dalle Donne and Hame was applied to experiments with bundles with spacer grids (Equation (2) and (3)) with non uniform radial heat flux distribution [8,9,11] and to other experiments with bundles supported by spiral wires [12,13,14,15] (Equation (2), (4), (5) and (6)) with reasonable results[6].

III. COMPARISON OF THE CHF-KFK-2 CORRELATION WITH NEW EXPERIMENTAL DATA

III.A. Experiments with Bundles with Grid Spacers

III.A.1 CEA Experiments

In 1988 M. Courtaud et al. of the Commissariat à l'Energie Atomique (CEA) published the results of their CHF experiments[16]. The experiments were performed with Freon-12 and transformed to equivalent water values using the transformation factors suggested by Stevens et al.[17] and by their own experiments. Table II shows the main data of the CEA experiments. Among others, they used also the CHF-KFK-2 correlation (Equations (2) and (3)) for the evaluation of their experiments. The agreement was rather good, the CHF-KFK-2 correlation underpredicting the experimental data of 8.2% with a standard deviation of.9.4%. However, the KfK correlation underpredicted of about 24% the results for a rod cluster with guide tube cells. This is to be expected as this correlation has been developed for uniform rod clusters. On the other hand, the application of the KfK correlation for the predicton of the DNBR (minimum ratio between the CHF and the maximum hot channel heat flux) in the reactor core is still valid, because there will certainly be a region in the large fuel rod bundles of a APWR which is practically unaffected by the presence of gu de tubes. Moreover, in the guide tube region the CHF is higher than predicted by the KfK correlation and the DNBR is determined by the bundle region unaffectec by the guide tubes.

III.A.2 JAERI Experiments

In 1989 Sugimoto et al. of Japan Atomic Energy Research Institute (JAERI) have published the results of their CHF water experiments with a 4 rod bundle[18]. Due to the relatively low number of rods and the considerable effects of the cluster boundaries, the results of the experiments were also evaluated in terms of local subchannel conditions using the COBRA-IV-I subchannel code. Besides with the CHF-KFK-2 correlation[6], the experiments were compared with the EPRI-B&W[19], EPRI-Columbia[20] and Katto[21] CHF correlations as well. Using the bundle averaged flow conditions, the two latter correlations overpredicted the experimental data by 20 to 100%. Therefore the comparison with the local conditions calculated with COBRA-IV-I was performed only for the first two correlations, which already

for the averaged flow conditions gave an agreement better than ± 20%. For the case of the KFK correlation, the unbalance factor Y' was used for the comparison with local flow conditions. By this evaluation method the CHF-KFK-2 correlation predicted the experimental data better than the EPRI-B&W correlation[18].

Subsequently JAERI performed other experiments with 4 and 7 rods[22]. Table III shows the main operating conditions of this experiment and of these of Ref.18. Based on the local flow conditions obtained with the subchannel analysis code COBRA-IV-I, the CHF-KFK-2 correlation[6] agreed with the experimental data within + 15% and -20% (see Fig.1), while the WSC-2, EPRI-B&W, EPRI-Columbia and Katto correlations failed to give a satisfactory agreement.

III.A.3 Mitsubishi Experiments

Mitsubishi has preformed CHF experiments with a 7 rod bundle with Freon-12 and water[23]. Table IV shows the main operating conditions of this experiment. Using the local flow conditions and the local subchannel unbalance factor, the experimental results agree quite well with the CHF-KFK-2 correlation for heat fluxes up to 2000 KW/m^2. For higher heat fluxes the CHF-KFK-2 correlation overpredicts the experimental data (18% at a flux of 4000 KW/m^2).

III.A.4 Experiment at KfK-Braunschweig University

The Karlsruhe Nuclear Center and the Braunschweig University have performed a joint experiment with a 7 rod bundle and Freon-12 (Ref.24). Table V shows the main operating conditions of this experiment. The data have been evaluated using local flow conditions calculated by means of the computer code COBRA-TUBS and applying the unbalance factor Y'. Within its range of application ($0.05 \times 10^6 < G < 4.09 \times 10^6$ Btu/hft^2 i.e. $70 < G < 5500$ kg/m^{2}s) the CHF-KFK-2 correlation underpredicts the experimental values of about 13%. Some uncertainty in the comparison may come from the use of the Ahmad scaling law[25]. Courtaud et al.[16] state that for rod bundles and high pressures the scaling factor for the mass velocity ($K = G_{water}/G_{freon}$) approaches the value 1, while Ahmad would predict 1.37. Also Akiyama et al[23] show that the factor K is equal one for a bundle geometry and high water pressures (>12.3 MPa). The Ahmad scaling law has been tested for a rod bundle for pressures up to 8 MPa and mass velocities up to 2800 kg/m^{2}s (Ref.26).

III.A.5 Experiments at Siemens-KWU

Recently Siemens-KWU has performed an experiment with a 37 rod bundle with water[27]. The 37 rods were arranged in a regular triangular array and contained in a hexagonal shroud. The careful choice of the shroud dimensions has made possible to have a factor F_G very near to one ($F_G = 1.0393$). The central seven rods have a power which is slightly higher than in the others, thus ensuring that the CHF occurs at the central rods. The relatively large number of rods and the care in the choice of geometrical parameters diminish the uncertainties in the process of trying to eliminate the shroud border effects. Also the chosen physical parameters are very relevant to the APWR application (see Table VI). The choice of water at high pressure and mass velocity, which involves the use of a very high heating power, practically eliminates the extrapolation to conditions which prevail in a APWR core. The use of water eliminates the uncertainties connected with the application of the scaling laws due to the use of Freon-12. This experiment is very valuable for the testing of the CHF-KFK-2 correlation.

The Siemens-KWU experimental data were compared with the CHF-KFK-2 correlation with the method illustrated in Ref.6. Although the geometrical value of F_G is 1.0393, the value $F_G = 1$ was used in the calculation, because the temperature of the water in the wall and corner subchannels is lower and the water density higher than in the central subchannels of the bundle. If the differences in water densities are accounted for, F_G becomes practically equal to 1.

Fig.2 shows the result of the comparison in the form $\Psi = \Phi_{comp.} / \Phi_{exp.}$ versus the mass velocity G (the dotted region is one standard deviation wide). The agreement between computed and experimental values is quite good (mean error = 3.38% and standard deviation = 6.07%), however the CHF-KFK-2 correlation tends to overpredict the CHF at high values of the mass velocity. We will deal with this problem in the Chapter IV.

III.B. Experimenta with Bundles with Six Integral Spiral Ribs

The CHF-KFK-2 correlation has been developed also for rod clusters with spiral wire supports (Equations (2), (4), (5) and (6)). However, the proposed APWR's with very tight lattices ($p/d < 1.2$) have the fuel rods supported by six integral spiral ribs

rather than by spiral wire[1]. This kind of support offers some advantages in respect to spiral wires, as, for a given axial distance between the supporting sections of the rods, the pressure drops are considerably smaller. This is because, in the case of six spiral starts, the axial pitch of the spiral is only 1/6th of the single start spiral wire for a given axial distance between the supporting sections. At the time of the development of the CHF-KFK-2 correlation, no CHF experiment with clusters with six integral spiral ribs was available in the literature. However, recently such an experiment has been performed by Siemens-KWU[28]. As in the case of the rod bundle with spacer grids (see Section III.A.5), due to the large number of rods and the operation up to high water pressures and mass velocities this experiment is very valuable for the testing of the CHF-KFK-2 correlation. Table VII shows the main operating conditions of this experiment with water.

Fig.3 shows a comparison of the KWU experimental data with the CHF-KFK-2 correlation for spiral wire spacers (Eqs.(2);(4),(5) and (6)). The correlation underpredicts the data by up to 40%. As the discrepancy increases with the water mass velocity, it is likely that this is due to wrong values for the parameter V, which accounts for the effect of the spacer on the CHF and is mass velocity dependent (Eq.(4)). The reason for this discrepancy is due to the fact that the correction factor FF in Eq. (4) has been obtained on the assumption that the increase of CHF caused by the spacer is proportional to the increase of the friction factor caused by the wire spiral spacer. This has been proved to be so for the single wire spiral supports[6], but it is not true when the results are applied to a different geometry as the six integral spiral ribs kind of support.

IV. IMPROVEMENTS TO THE CHF-KFK-2 CORRELATION IN VIEW OF THE SIEMENS-KWU EXPERIMENTS

IV.A Bundles with Grid Spacers

The critical heat flux correlation CHF-KFK-2 is based on experimental data with mass velocities values up to 4.09×10^6 lb/ft^{2}h (= 5550 kg/m^{2}s), however only three experimental points were available for mass velocities above 3.2×10^6 lb/ft^{2}h (see Fig.1 of Ref.6). The experiments at Siemens-KWU extend to mass velocity values of 4.4×10^6 lb/ft^{2}h (= 6000 kg/m^{2}s), furthermore 39 experimental points are available for mass velocities above 3.2×10^6 lb/ft^{2}h (see Fig.2). On the base of these reliable data is thus possible to improve the CHF-KFK-2 correlation in the range of high mass velocities. Fig.4 shows the V values versus the mass velocity G. These V values have been calculated with the Q values of Eq. (2) and the experimental values of the CHF. Plotted in Fig.4 is also Eq.(3) which is used in the correlation CHF-KFK-2. From the figure it is evident that Eq. (3) underpredicts the V values for $G > 3 \times 10^6$ lb/ft^{2}h. This corresponds to the fact that the CHF-KFK-2 correlation overpredicts the experimental data at these high G values (Fig.2), as low values of V mean high CHF values. Fig.5 shows the same experimental data, compared with a new correlation for V, namely:

$$V = -0.252 - 2.789\, e^{-3.874G} + 1.915 e^{-0.234\,G} \qquad \text{for } G \leq 3.5 \tag{7}$$

$$V = 0.59 \qquad \text{for } G > 3.5$$

Eq.(7) is identical to Eq.(3), but it assumes that V is constant for G above 3.5×10^6 lb/ft^{2}h. This seems plausible as V accounts for the effects of the spacers on the CHF. It is known from the literature (see for instance Ref.29) that the drag coefficients for grid spacers decrease with the Reynolds number up to Reynolds numbers of about 10^5 and then tend to remain constant. As Reynolds numbers above 10^5 correspond roughly to G values greater than 3.5×10^6 lb/ft^{2}h, this would indicate that the improvement in the CHF caused by the spacer grids is directly connected to the value of the drag coefficients.

Fig.5 shows that the agreement between experimental values of V and those predicted by Eq. (7) is considerably better at high G values. Fig.6 shows the comparison of the experimental CHF-values with the calculated ones, using Eq. (7)

in place of Eq. (3). The agreement is now considerably better, the mean error being 0.95% and the standard deviation 4.95%.

IV.B. Bundles with Six Integral Spiral Ribs

In Section III.B we have seen that the CHF-KFK-2 correlation for spiral wire supports cannot predict properly the experimental data obtained by Siemens-KWU for a bundle with six integral spiral ribs. We tried therefore another approach.

Fig.7 shows the result of the comparison between calculation and the experiments of the bundle with six integral spiral ribs. The calculated critical heat flux values have been computed using the CHF-KFK-2 correlation for spiral wire spacers (Eq.(2) and (4)), however the value of V has been obtained with the factor FF set equal to one. The figure shows that the agreement between experiment and calculation is excellent, the mean error being 0.9% and the standard deviation 5.6%. This means that the results with the experiments with six integral spiral ribs (H/d = 63.2, where H = axial pitch of the spiral rib, d = rod diameter) agree quite well with those for the bundle with the single spiral wire for which Eq. (4) (with FF = 1) was obtained. This was a bundle with H/d = 13.64 and p/d = 1.05 (see Ref. /6/). If one assumes that the effects of the geometrical parameters p/d and H/d on the critical heat flux are the same for the case with six spiral ribs as for the case with one single spiral wire, it is possible to account for the different number of starts between a single wire and a six spiral ribs kind of support. Eq. (6) should be replaced by:

$$F = \left(\frac{p}{d}\right)^{0.5} + n_s^{1.58} \left[7.6 \; \frac{(p/d)^3}{H/d} \right]^{2.16} \qquad (8)$$

Whereby n_s, number of starts, is equal 1 for the single wire case and equal to 6 for the six integral spiral ribs case respectively. Eq. (8) should, however, used with caution, as it is based on only one experiment with a rod cluster with six spiral ribs.

V. CONCLUSIONS

The critical heat flux correlation developed at KfK for the central rods (not affected by the shroud walls) of tight lattice triangular array clusters has been improved by comparison with recently performed CHF experiments. Especially the experiments performed at Siemens-KWU were useful for the improvement and extension of the CHF correlation. This is because these experiments were performed with a relatively large number of rods and up to high values of water pressure and mass flow.

As the previous ones, the new CHF-KFK-3 correlation is based on the WSC-2 correlation (Table I). This means that, when the rods are affected by the shroud wall of the cluster, as in the case of clusters with a small number of rods, or in presence of strong power gradients perpendicular to the water flow, a subchannel analysis of the data with a COBRA-type computer code should be performed and the parameter Y' applied. The cluster geometry relevant parameters remain for the CHF-KFK-3 correlation the same as for the previous CHF-KFK-2 correlation, namely:

$Q_1 = 1.748$, $Q_2 = 7.540$, $Q_3 = -1$, $Q_4 = 8.783$

However, the parameter V, which accounts for the effect of the spacers on the CHF, has been changed as follows:
For clusters with grid spacers:

$$V = -0.252 - 2.789 \exp(-3.874G) + 1.915 \exp(-0.234G) \qquad \text{for } G \leqslant 3.5$$

$$V = 0.59 \qquad \text{for } G > 3.5$$

And for clusters with spiral supports:

$$V = 1 - FF\,(0.336 + 0.09G - 0.697 \exp(-2.68\,G))$$

where $FF = 2.6695\,(F^{0.915} - 1)$

and $$F = \left(\frac{p}{d}\right)^{0.5} + n_s^{1.58} \left[7.6\,\frac{(p/d)^3}{H/d}\right]^{2.16}$$

Whereby n_s, number of starts, is equal 1 for the single wire support and equal to 6 for the six integral spiral ribs support respectively. In the case of the six integral

spiral ribs the correlation should be used with caution as it based on the only one geometry (n_s = 6, p/d = 1.116, H/d = 63.2) which has been tested so far.

The validity range of te present correlation is determined by the experimental evidence on which the correlation is based. This is given by the experimental data on which the CHF-KFK-2 correlation was based (see Ref.6) plus the two recent Siemens-KWU experiments [27,28]. Table VIII summarizes the validity range of the proposed CHF-KFK-3 correlation.

APPENDIX

Conversion factors:

G, 10^6 lb/h ft^2 = 1356 kg/m^{2}s

D_h,Z, 1 in. = 0.0254 m

p, 1 psia = 0.006893 MPa

ΔH, λ, 1 Btu/lb = 2325 J/kg

Φ, 10^6 Btu/ft^2 h = 3155 kW/m^2

NOMENCLATURE

e = $(\Phi_{comp} - \Phi_{exp}) / \Phi_{exp}$ = correlation error for an experimental point

d = rod diameter (in.)

D_h = hydraulic diameter of the rod cluster central coolant channel (in.)

F = $\left(\frac{p}{d}\right)^{0.5} + n_s^{1.58} \left[7.6 \frac{(p/d)^3}{H/d}\right]^{2.16}$

correction factor taking into account the increase in the friction factor caused by spiral spacers

F_G = correction factor to obtain the mass velocity in the central coolant channels from the mass velocity averaged over the whole cluster

F_P = correction factor to account for the radial nonuniform power distribution

G = mass velocity (10^6xlb/h ft^2)

$\overline{G}$ = mass velocity averaged over the whole cluster (10^6xlb/hft^2)

H = axial pitch of the spiral spacers (in.)

ΔHi = inlet subcoolin (Btu/lb)

L = test section in the cluster (in.)

p = rod pitch in the cluster (in.)

p = pressure (psia)

Q_1, Q_2, Q_3, Q_4 = geometry-dependent factors in the CHF correlation

V = parameter that accounts for the effect of the spacers on the CHF

X = steam quality

Z = distance from channel inlet to the point where the CHF occurs (in.)

ε_{RMS} = root-mean-square error

Φ, Φ_{CHF} = critical heat flux (10^6 Btu/hft^2)

λ = latent heat of vaporization (Btu/lb)

Ψ = $(\Phi_{comp} / \Phi_{exp})$

Subscripts

comp = computed

exp = experimental

CHF = at the axial section where the CHF occurs

REFERENCES

1. C.H.M. BROEDERS and M. DALLE DONNE, "Conceptual Design of a $(P,U)O_2$ Core with a Tight Fuel Rod Lattice for an Advanced Pressurized Light Water Reactor", Nuclear Technology, 71, 82 (1985).

2. H. MOLDASCHL, R. BROGLI and B. KUCZERA, "Status and Prospects of the Cooperative KWU High Converter Development 1989", Proc. 5th Int. Conf. Emerging Nuclear Energy Systems, Karlsruhe, July 3-6, 1989, p.25, World Scientific (1989).

3. C.H.M. BROEDERS and M. DALLE DONNE, "Neutron physics and Thermohydraulics Design of a Reference High Conversion Reactor", IAEA T.C. Meeting on Technical and Economic Aspects of High Converters, Nürnberg, Germany, 26-29 March 1990.

4. Proc. of Advanced Light and Heavy Water Reactors for Improved Fuel Utilisation", Vienna 26-29 November 1984, IAEA-TECDOC-344 (1985).

5. M. DALLE DONNE and W. HAME, "A Critical Heat Flux Correlation for Advanced Pressurized Light Water Reactor Application," KfK-3279, EUR-7057e, Kernforschungszentrum Karlsruhe (1982).

6. M. DALLE DONNE and W. HAME, "Critical Heat Flux Correlation for Triangular Arrays of Rod Bundles with Tight Lattices, including the Spiral Spacer Effect", Nuclear Technology, 71, 111 (1985).

7. R.W. BOWRING, "WSC-2, A Subchannel Dryout Correlation for Water-Cooled Clusters over the Pressure Range 3.4-15.9 MPA," AEEW-R983, U.K. Atomic Energy Authority (1979).

8. B.W. LETOURNEAU et al., "Critical Heat Flux and Pressure Drop Tests with Parallel Upflow of High Pressure Water in Bundles of Twenty 0.25 and 0.28 in Diameter Rods," WAPD-TM-1013, Westinghouse Electric Corporation (1975).

9. B.W. LETOURNEAU et al., "Critical Heat Flux and Pressure Drop Tests with Parallel Upflow of High Pressure Water in Bundles of Twenty 3/4-in. Rods," Nucl. Sci. Eng., **54**, 214 (1974).

10. B. MATZNER, "Heat Transfer and Hydraulic Studies for SNAP-4 Fuel Element Geometries," TID-19563, Columbia University, Engineering Research Laboratories (Sept. 1963).

11. K.J. COELING, "Critical Heat Flux and Pressure Drop Tests with Vertical Upflow of Water in a 20-Rod Bundle of 0.69 in. Diameter Rods," WAPD-TM-1155, Westinghouse Electric Corporation (1977).

12. B. MATZNER and J.S. NEILL, "Forced Flow Boiling in Rod Bundles at High Pressure", DP-857, TID-4500, U.S. Atomic Energy Commission (Sept. 1963).

13. E.D. WATERS et al., "Boiling Burnout Experiments with 19-Rod Bundles in Axial Flow," HW-77303, Hanford Engineering Development Laboratory / General Electric Company (Aug. 1963).

14. L.S. TONG et al., "Critical Heat Flux (DNB) in Square and Triangular Array Rod Bundles," JSME Semi-International Symposium, September 4-8, 1967 Tokyo.

15. R.V. MACBETH, "Burn-Out Analysis. Part 5: Examination of Published World Data for Rod Bundles," AEEW-R358, U.K. Atomic Energy Authority (1964).

16. M. COURTAUD, R. DERUAZ and L. GROS D'AILLON, "The French Thermal-Hydraulic Program Addressing the Requirements of Future Pressurized Water Reactors", Nuclear Technology, 80, 73 (1988).

17. G.F. STEVENS et al., "A Comparison between Burnout Data for 19 Rod Cluster Test Sections Cooled by Freon-12 at 155 psia and by Water at 1000 psia in Vertical Upflow", AEEW-R468, U.K. Atomic Energy Authority (1966).

18. J. SUGIMOTO, T. IWAMURA, T. OKUBO and Y. MURAO, "Thermal-hydraulic Study on High Conversion Light Water Reactor at JAERI", Proc. 4th Int. Meet. Nuclear Reactor Thermal-Hydraulics, Vol.2, 799, Karlsruhe, Germany, 10-13 Oct. 1989, Verlag G. Braun, Karlsruhe.

19. V.O. UOTINEN et al., "Technical Feasibility of a Pressurized Water Reactor Design with a Low-Water Fraction Lattice", EPRI-NP-1833 (1981).

20. D.G. REDDY and C.F. FIGHETTI, "Parametric Study of CHF Data, A Generalized Subchannel CHF Correlation for PWR and DWR Fuel Assemblies", EPRI-NP-2609, Vol.2 (1983).

21. Y. KATTO, "General Features of CHF of Forced Convection Boiling in Uniformly Heated Rectangular Channels, Int. J. Heat Mass Transfer, 24, 1413 (1981).

22. T. IWAMURA, T. OKUBO, T. SUEMURA, F. HIRAGA and Y. MURAO, "Critical Heat Flux Experiments for High Conversion Light Water Reactor", JEARI-M 90-044, Japan Atomic Energy Research Institute (1990), in Japanese.

23. Y. AKIYAMA, K. HORI and S. TSUDA, "DNB Experiments for High Conversion PWR Core Design", to be published in Nuclear Science and Engineering, see also Proc. 4th Int. Meet. Nuclear Reactor Thermal-Hydraulics, Vol.2, 788, Karlsruhe, Germany 10-13 Oct. 1989, Verlag G. Braun, Karlsruhe.

24. W. ZEGGEL and F.J. ERBACHER, "Experimental Investigation on CHF of Tight-Lattice PWR's", IAEA Meeting on Technical and Economic Aspects of High Converters, Nuremberg, 26-29 March 1990, IAEA-TECDOC-700 (1990)

25. S.Y. AHMAD, "Fluid to Fluid Modeling of Critical Heat Flux: A Compensated Distorsion Model," Int. J. Heat Mass Transfer, 16, 641 (1973).

26. G.D. MCPHERSON and S.Y. AHMAD, "Fluid Modeling of Critical Heat Flux in an 18-Element Bundle, Nucl. Engng. Design 17, 409 (1971).

27. U. SIMON, unpublished, Siemens-KWU, 1990.

28. U. SIMON, unpublished, Siemens-KWU, 1988.

29. K. REHME, "Pressure Drop Correlations for Fuel Elements Spacers", Nuclear Technology, 17, 15 (1973).

Table I: WSC-2 correlation

$$\Phi(x10^6 \text{ Btu/hr ft}^2) = \frac{A+B\Delta H_i}{C+ZYY'}$$

$$A = \frac{0.25\ GD\lambda F_1 Q_1}{1+Q_2F_2GD(Y')^{Q_3}} \qquad B = 0.25\ GD$$

$$C' = \frac{Q_4F_3\sqrt{GDY'}}{D_h} \qquad C = C'V\left[1 + \frac{Y-1}{1+G}\right]$$

where: $D=F_pD_h$; D_h=coolant channel hydraulic diameter (in)

F_p = radial form factor in the considered section of the bundle subchannel

$p_r = 10^{-3}\ p$ p=pressure (p.s.i.a.)

$F_1=p_r^{0.982}\ e^{1.17\ (1-p_r)}$

$F_2=p_r^{0.841}\ e^{1.424\ (1-p_r)}$

$F_3=p_r^{1.851}\ e^{1.241\ (1-p_r)}$

G = mass velocity (10^6 lb/ft²hr)

λ = latent heat of evaporation (Btu/lb)

ΔH_i = inlet subcooling (Btu/lb)

z = distance from channel inlet (in)

Y = ratio of average cluster heat flux from entry to z to local cluster radial-average heat flux at z

Y'= inbalance factor, ratio of the enthalpy increase in the considered subchannel to the heat produced in the subchannel from entry to z

V = grid spacers parameter. For the best fit of experimental data V=0.7.

geometry parameter	Q_1	Q_2	Q_3	Q_4
triangular array	1.329	2.372	-1	12.26

Table II: CEA CFH Experiments[16]. Range of Operating Conditions

Number of rods = 19
Rod diameter = 8.65 and 9.5 mm
Rod pitch = 9.96 and 12.23 mm
p/d = 1.151 and 1.287
Pressure = 7.6 to 16 MPa
Mass velocity = 2000 to 8000 kg/m²s
Exit steam quality = -0.2 to 0.4
Heat Flux = 500 to 3800 KW/m²

} equivalent water

Table III: JEARI CHF Experiments[18,22]. Range of Operating Conditions

Number of rods = 4 and 7
Rod diameter = 9.5 mm
Rod pitch = 10.7 and 11.4 mm
p/d = 1.126 and 1.2
Pressure = 1 to 3.9 MPa
Mass velocity = 460 to 4270 kg/m²s
Exit steam quality = 0.02 to 0.35
Heat flux = 700 to 4700 KW/m²

Table IV: Mitsubishi CHF Experiments[23]. Range of Operating Conditions

Number of rods = 4
Rod diameter = 9.5 mm
Rod pitch = 12 mm
p/d = 1.263
Pressure = 2-2.9 MPa
Mass velocity = 1900 - 3600 kg/m²sec } with Freon 12
Inlet subcooling = 3-36 K
Pressure = 12.3 - 16.7 MPa
Mass velocity = 2800-4900 kg/m²sec } with water
Inlet subcooling = 20-170 K

Table V: KfK-Braunschweig Experiments[24]. Range of Operating Conditions

Number of rods = 7
Rod diameter = 9.5 mm
Rod pitch = 10.9 mm
p/d = 1.147
Pressure = 2.3 MPa
Mass velocity = 1000-6000 kg/m²sec } with Freon 12
Exit steam quality = -0.34 ÷ +0.09
Heat flux = 100 - 500 KW/m²

Table VI: Siemens-KWU CHF experiment with grid spacers[27]
Range of operating conditions

Number of rods = 37

Rod diameter = 9.0 mm

Rod pitch = 10.6

p/d = 1.178

Test section length = 1.2 m

Pressure = 7 - 16 MPa

Mass velocity = 200 - 6000 kg/m²s

Exit steam quality = -0.521 ÷ +0.263

Table VII: Siemens-KWU CHF experiment with six spiral ribs cluster[28].
Range of operating conditions

Number of rods = 37

Rod diameter = 9.5 mm

Rod pitch = 10.6 mm

p/d = 1.116

Test section length = 1.2 m

Axial pitch of the spiral ribs = 600 mm

Pressure = 7-16 MPa

Mass velocity = 1000 - 7000 kg/m²s

Exit steam quality = -0.53 ÷ 0.09

Table VIII: Validity range of the CHF-KFK-3 correlation
(central rods, unaffected by shroud walls, triangular rod array)

1. Grid spacers

pitch to rod diameter ratio = 1.02 ÷ 1.36
pressure = 2.9 ÷ 16 MPa = 400 ÷ 2320 p.s.i.a
mass velocity = 70 ÷ 6000 kg/m²s = 0.05×10^6 ÷ 4.4×10^6 lb/h·ft²
steam quality at CHF section = -0.52 ÷ 0.96

2. Single wire spacers

pitch to rod diameter ratio = 1.05 ÷ 1.41
wire axial pitch to rod diameter ratio = 13.5 ÷ 35.5
pressure = 7-10 MPa = 1000 ÷ 1500 p.s.i.a
mass velocity = 650 ÷ 5550 kg/m²s = 0.48×10^6 ÷ 4.1×10^6 lb/h·ft²
steam quality at CHF section = -0.04 ÷ 0.53

3. Six spiral integral ribs spacers

pitch to rod diameter ratio = 1.116
rib axial pitch to rod diameter ratio = 63.2
pressure = 7 ÷ 16 MPa = 1000 ÷ 2320 p.s.i.a
mass velocity = 1000 ÷ 7000 kg/m²s = 0.74×10^6 ÷ 5.2×10^6 lb/h·ft²
steam quality at CHF section = -0.53 ÷ 0.09

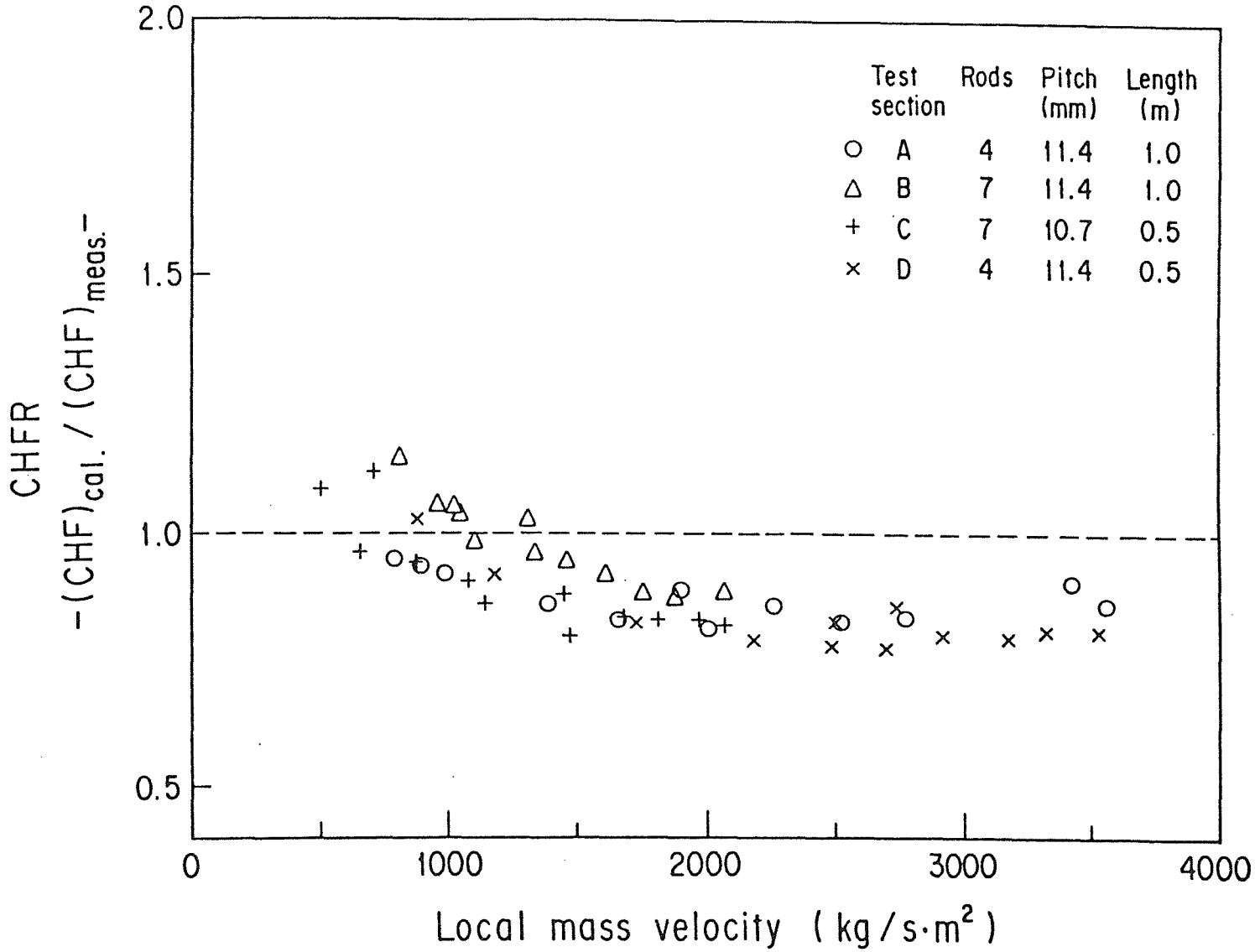

Fig.1. JAERI experiments with 4 and 7 rods. Comparison of the experimental data with the prediction of the CHF-KFK-2 correlation. The experimental data have been analyzed with the subchannel code COBRA-IV-I. The unbalance factor Y' has been applied (from Ref. 22).

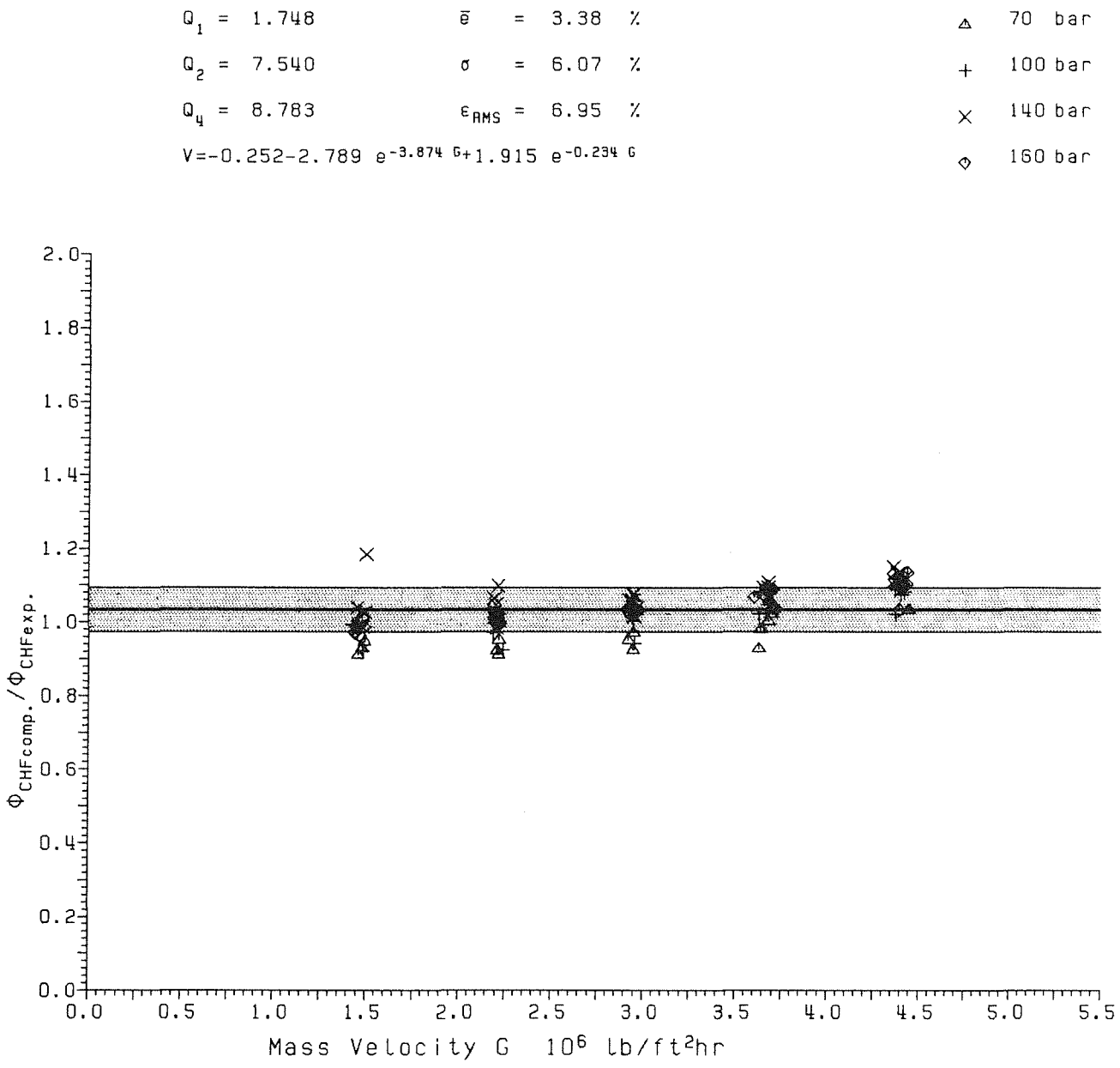

Fig.2. Siemens-KWU experiments with grid spacers. Comparison of the experimental data with the prediction of the CHF-KFK-2 correlation.

Q_1 = 1.748 $\quad \bar{e}$ = -30.10%

Q_2 = 7.540 $\quad \sigma$ = 8.90 %

Q_4 = 8.783 $\quad \varepsilon_{RMS}$ = 31.39 %

$V = 1\text{-}FF\,(0.336+0.09\,G-0.697\,e^{-2.68\,G})$

△ 70 bar
+ 100 bar
× 140 bar
◇ 160 bar

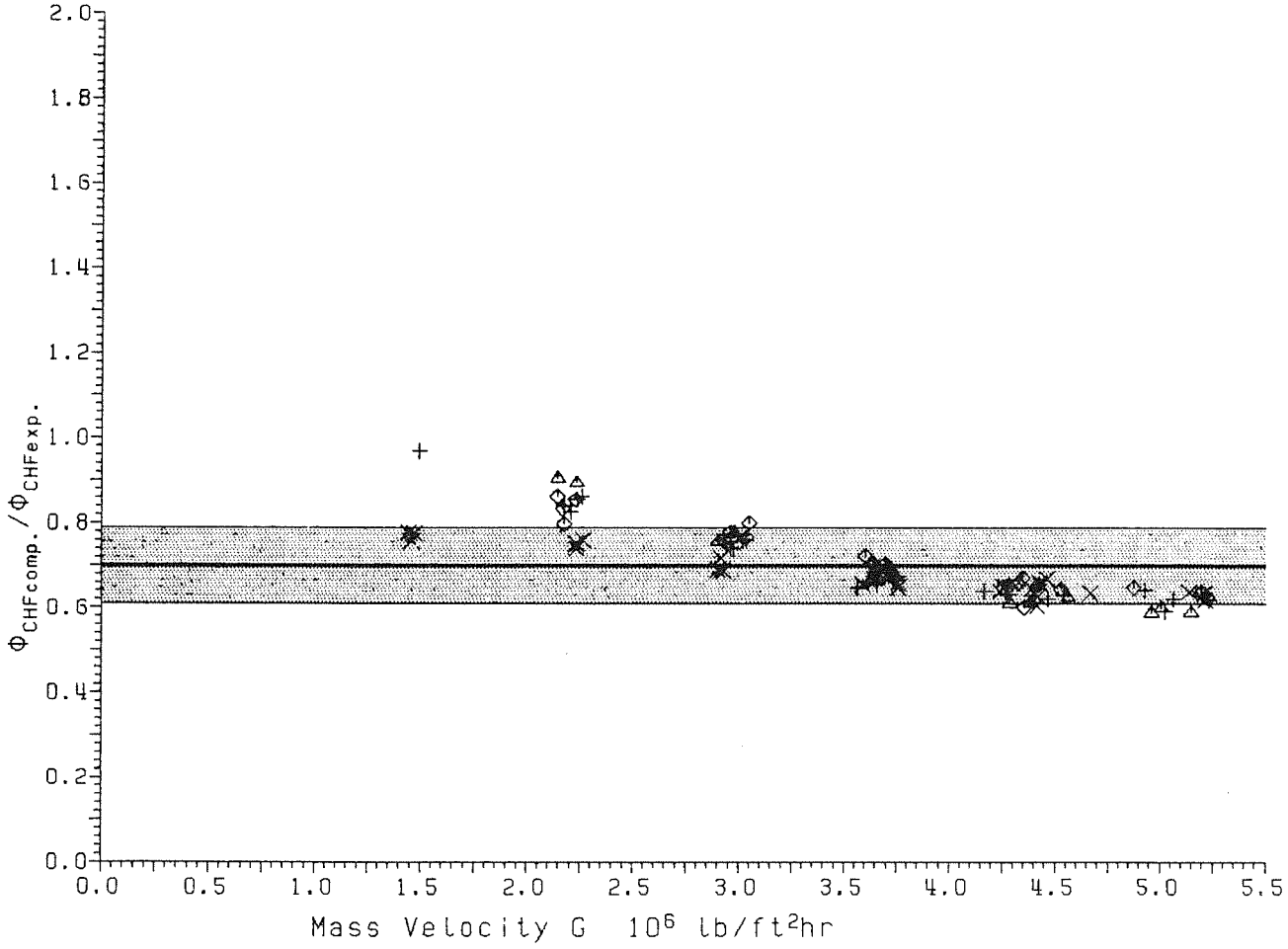

Fig.3. Siemens-KWU experiments with six integral spiral ribs. Comparison of the experimental data with the prediction of the CHF-KFK-2 correlation.

$Q_1 = 1.748$

$Q_2 = 7.540$

$Q_4 = 8.783$

$V = -0.252 - 2.789\ e^{-3.874\ G} + 1.915\ e^{-0.234\ G}$

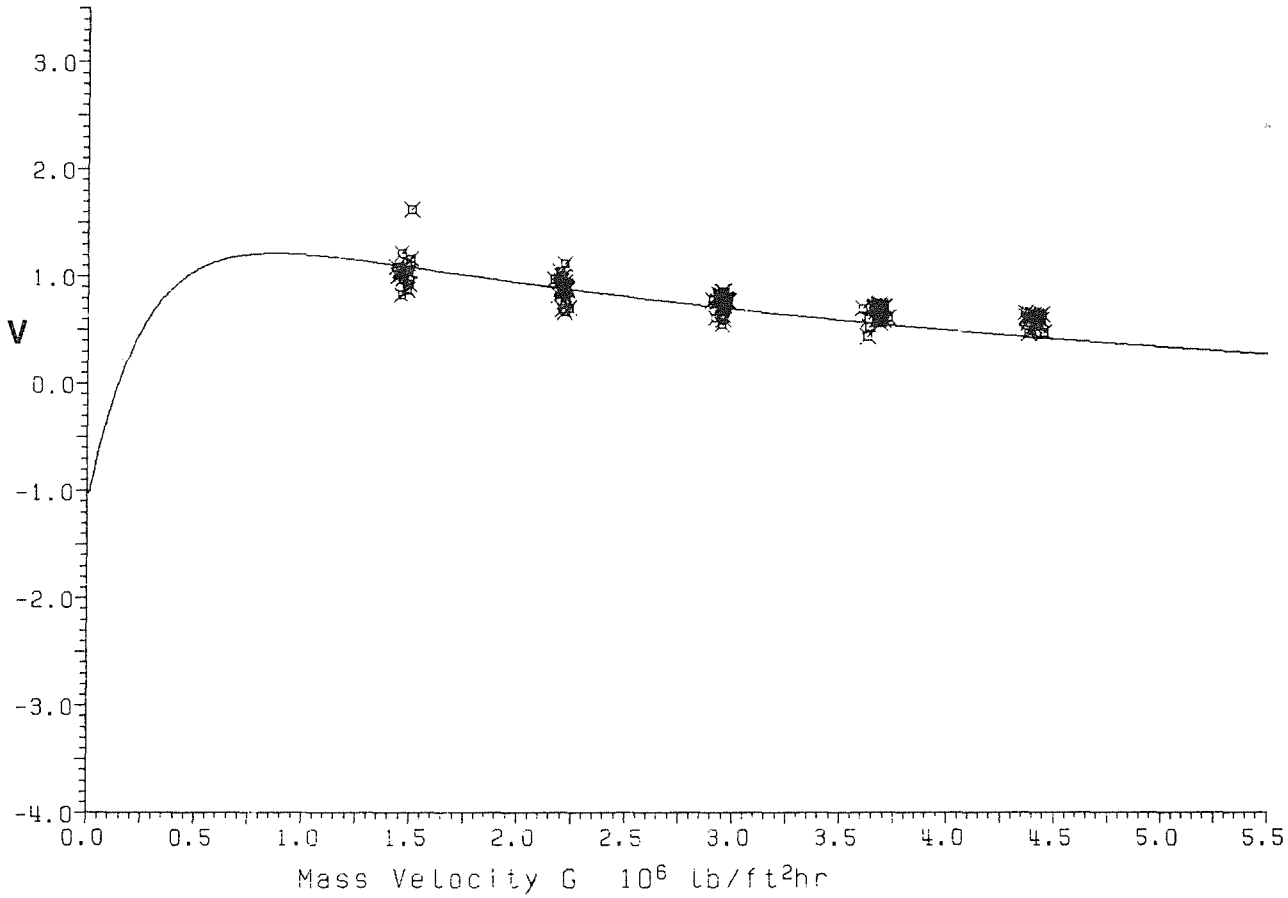

Fig.4. Siemens-KWU grid spacer data: V versus G for the Q values of Eq. (2) and $\Phi_{CHF} = \Phi_{CHF\ exp.}$. Comparison with the V values given by Eq. (3).

$Q_1 = 1.748$

$Q_2 = 7.540$

$Q_4 = 8.783$

if G<3.5 $\quad V=-0.252-2.789\ e^{-3.874\ G}+1.915\ e^{-0.234\ G}$

if G>3.5 $\quad V=0.59$

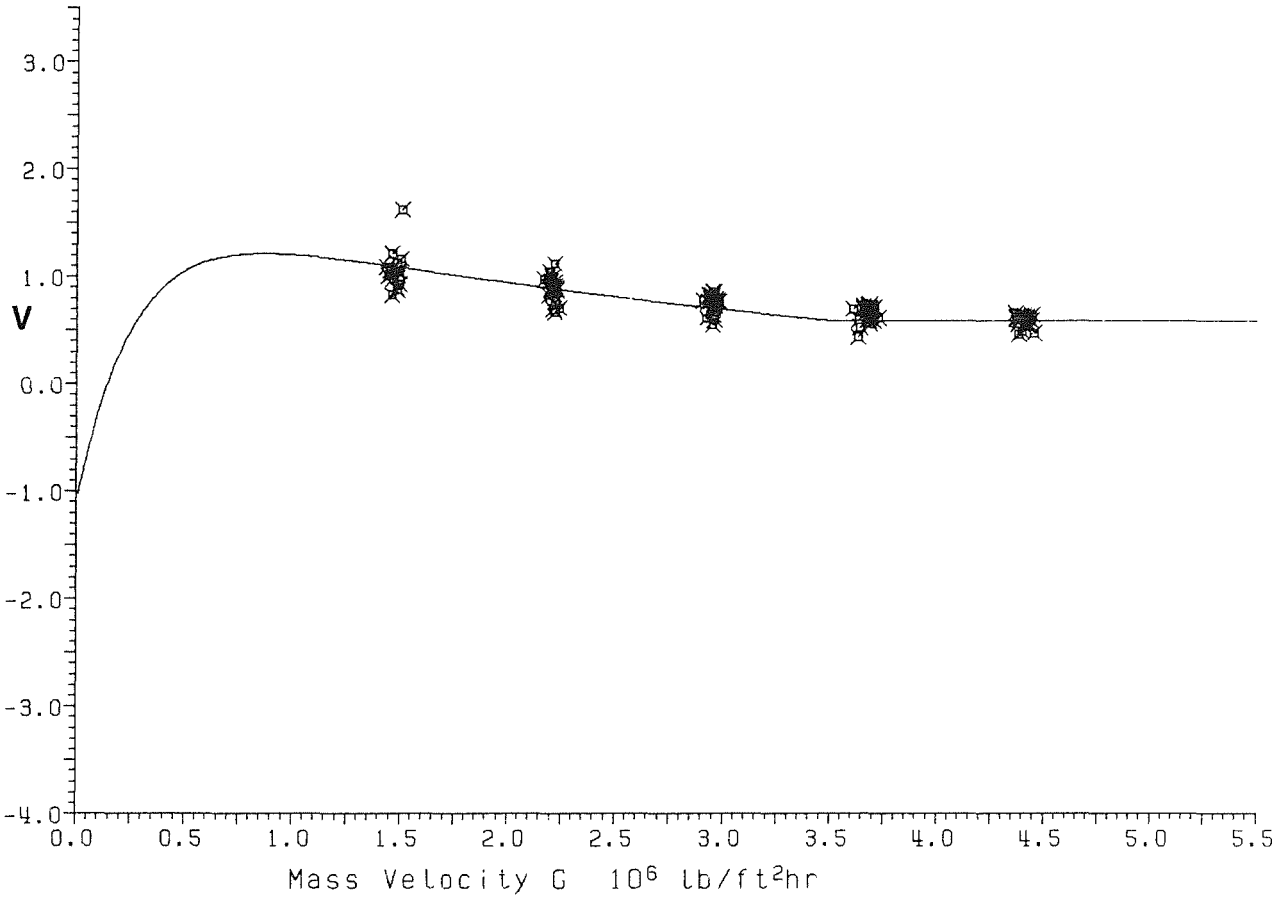

Fig.5. Siemens-KWU grid spacer data: V versus G for the Q values of Eq. (2) and $\Phi_{CHF} = \Phi_{CHF\ exp.}$. Comparison with the V values given by Eq. (7) (CHF-KFK-3 correlation).

Q_1 = 1.748 $\quad \bar{e}$ = 0.95 % $\quad$ △ 70 bar

Q_2 = 7.540 $\quad \sigma$ = 4.95 % $\quad$ + 100 bar

Q_4 = 8.783 $\quad \varepsilon_{RMS}$ = 5.04 % $\quad$ × 140 bar

if G<3.5 $\quad V=-0.252-2.789\ e^{-3.874\ G}+1.915\ e^{-0.234\ G}$ $\quad$ ◇ 160 bar

if G>3.5 $\quad V=0.59$

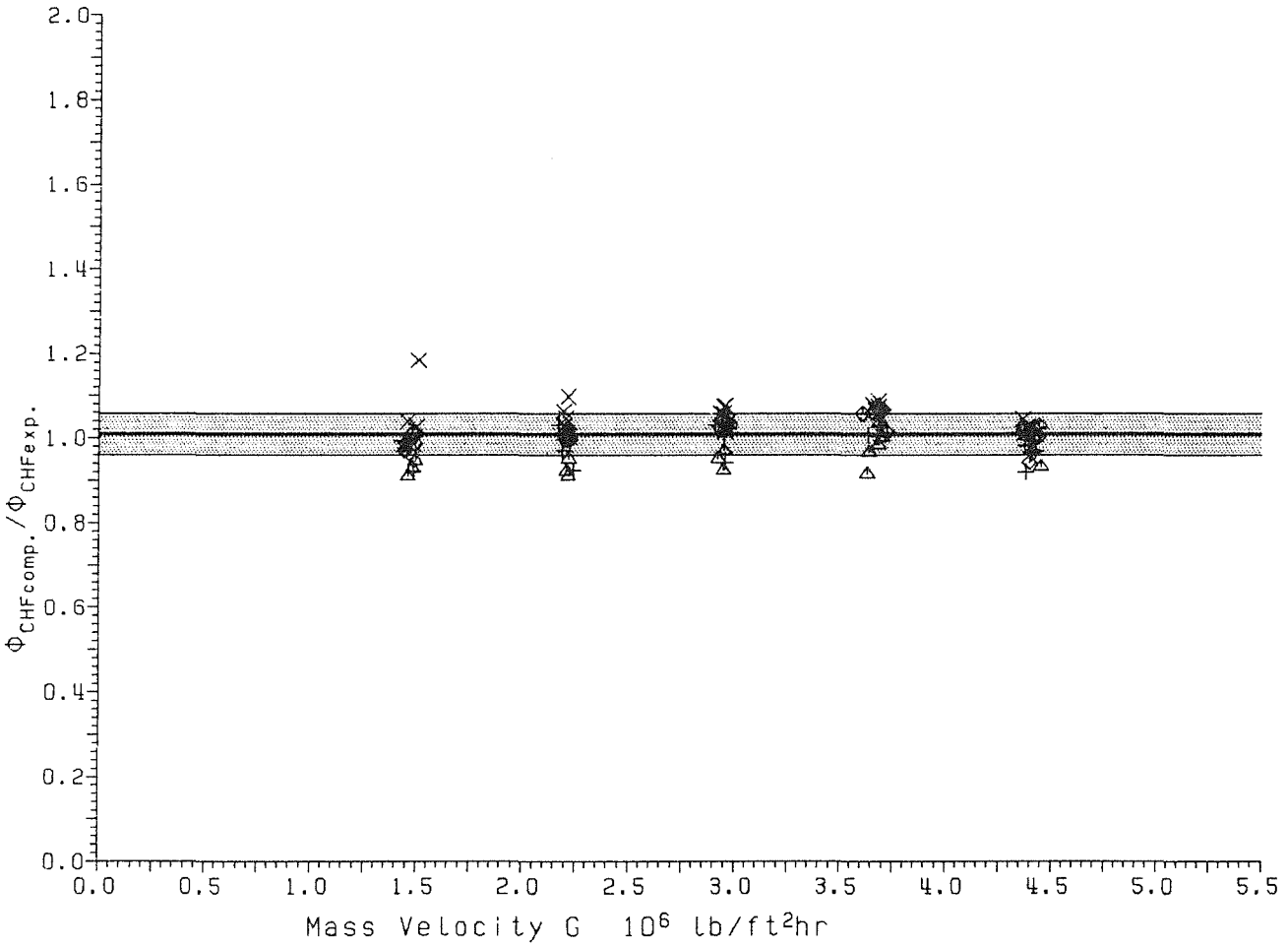

Fig.6. Siemens-KWU grid spacer data. Comparison of the experimental data with prediction of the CHF-KFK-3 correlation.

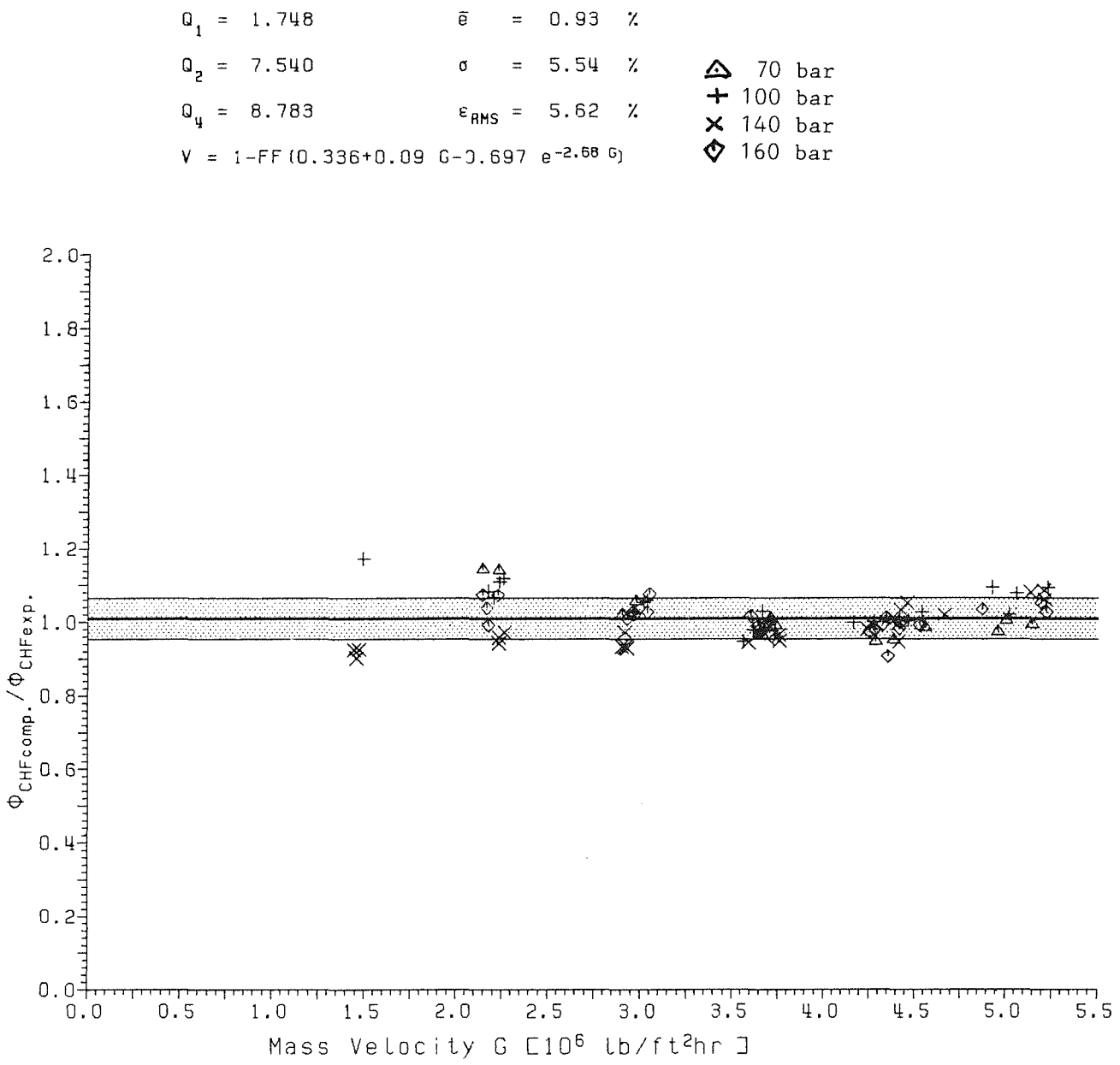

Fig.7. Siemens-KWU experiments with six integral spiral ribs. Comparison of the experimental data with the prediction of the CHF-KFK-3 correlation.